BJR

Received:
9 January 2014

Accepted:
3 March 2014

doi: 10.1259/bjr.20140065

Cite this article as:
Chowdhury R, Ganeshan B, Irshad S, Lawler K, Eisenblätter M, Milewicz H, et al. The use of molecular imaging combined with genomic techniques to understand the heterogeneity in cancer metastasis. Br J Radiol 2014;87:20140065.

REVIEW ARTICLE

The use of molecular imaging combined with genomic techniques to understand the heterogeneity in cancer metastasis

[1,2]R CHOWDHURY, MRCP(UK), BSc (Hons), [3]B GANESHAN, PhD, BEng Biomedical Engineering, [4]S IRSHAD, MRCP(UK), BSc, [1,5]K LAWLER, PhD, [1,6]M EISENBLÄTTER, MD, [7]H MILEWICZ, PhD, [8]M RODRIGUEZ-JUSTO, MB ChB, FRCPath, [3]K MILES, MD, FRCR, [2,9]P ELLIS, MD, FRACP, [3]A GROVES, MD, FRCR, [10,11]S PUNWANI, FRCR, PhD and [1,4,7,9]T NG, FMedSci, PhD

[1]Richard Dimbleby Department of Cancer Research, Randall Division of Cell and Molecular Biophysics, King's College London, London, UK
[2]Department of Medical Oncology, Guy's and St Thomas' NHS Foundation Trust, London, UK
[3]Institute of Nuclear Medicine, University College London Hospital, London, UK
[4]Breakthrough Breast Cancer Research Unit, Research Oncology, King's College London, Guy's Hospital, London, UK
[5]Institute for Mathematical and Molecular Biomedicine, Kings College London, Guy's Medical School Campus, London, UK
[6]Division of Imaging Sciences and Biomedical Engineering, School of Medicine, King's College London, The Rayne Institute/St Thomas' Hospital, London, UK
[7]UCL Cancer Institute, University College London, London, UK
[8]Department of Research Pathology, Faculty of Biomedical Sciences, University College London Medical School and University College London Hospitals, London, UK
[9]Division of Cancer Studies, King's College London, Guy's Medical School Campus, London, UK
[10]Division of Imaging, University College London Hospital, London, UK
[11]Centre of Medical Imaging, University College London Hospital, London, UK

Address correspondence to: Professor Tony Ng
E-mail: *tony.ng@kcl.ac.uk*

Ruhe Chowdhury, Balaji Ganeshan and Sheeba Irshad have contributed equally to this article.

ABSTRACT

Tumour heterogeneity has, in recent times, come to play a vital role in how we understand and treat cancers; however, the clinical translation of this has lagged behind advances in research. Although significant advancements in oncological management have been made, personalized care remains an elusive goal. Inter- and intratumour heterogeneity, particularly in the clinical setting, has been difficult to quantify and therefore to treat. The histological quantification of heterogeneity of tumours can be a logistical and clinical challenge. The ability to examine not just the whole tumour but also all the molecular variations of metastatic disease in a patient is obviously difficult with current histological techniques. Advances in imaging techniques and novel applications, alongside our understanding of tumour heterogeneity, have opened up a plethora of non-invasive biomarker potential to examine tumours, their heterogeneity and the clinical translation. This review will focus on how various imaging methods that allow for quantification of metastatic tumour heterogeneity, along with the potential of developing imaging, integrated with other *in vitro* diagnostic approaches such as genomics and exosome analyses, have the potential role as a non-invasive biomarker for guiding the treatment algorithm.

Although continual improvements in diagnosis, surgical techniques and radiation oncology have together provided improved survival for many forms of human cancers, a majority of deaths from cancer are caused by the development and continuous growth of metastases that are resistant to conventional therapies. Similarly, although the use of systemic non-targeted and targeted adjuvant therapies has helped to prevent the spread of tumour cells from the primary site and is now a standard practice for many tumour types, the emergence of resistant disease continues to be a significant cause of patient mortality. These features provide an insight into the dynamic nature of the signalling network within the tumour cells,[1] and human cancers are now being increasingly recognized as heterogeneous, characterized by distinct pathological, genomic, clinical and therapeutic features.

Nearly 150 years after the original theory of tumours originating from immature cells by Virchow,[2] innovative technological approaches unequivocally demonstrate the cellular

heterogeneity of tumours, composed of distinct subpopulations of cancer cells within ("intra") and between ("inter") tumours of individual patients. These subpopulations are characterized by specific genetic and morphological profiles, representing the clonal selection and evolution of that tumour.[3,4] This heterogeneity provides a powerful internal mechanism through which tumour cells can ultimately escape environmental stresses, including oncological therapies, posing a considerable challenge for translational researchers.

There is considerable evidence that the tumour microenvironment actively contributes to tumour heterogeneity.[5] Arguably the best example of this is the "pre-metastatic niche", defined as the creation of an ideal thriving environment for the primary tumour to "seed" to. Through the secretion of cytokines, chemokines and growth factors, the primary tumour "primes" a distal site to become an ideal niche/target organ, favourable for future metastatic colonization.[6] Although in some cases the target organ is already primed for metastatic spread and many organs may have "seeding" of cells, only a few will take "root".[7] Increasing understanding of tumour heterogeneity demands an effort from researchers to establish and understand pre-metastatic changes within distant organs and their major drivers.

This new paradigm of cancer heterogeneity has yet to be fully assimilated into everyday patient management. It has been well documented with certain cancers that imaging signals can show phenotypic tumour heterogeneity and have clinical implications; for example, in radio-iodine imaging of metastatic thyroid cancer, some metastatic lesions may not take up radio-iodine and therefore will be unaffected by radio-iodine therapy. However, for the majority of tumours, biopsies remain the standard of care for assessing tumour biology but cannot be expected to represent the entirety of a tumour in this tumour heterogenic era.[4] Many physicians advocate the re-biopsy of metastatic disease at re-presentation for histological analysis and comparison with the primary, in an attempt to improve the choice of therapy upon relapse, having taken into account, for instance, intertumoral heterogeneity between the primary and metastatic disease.[8] Repeated biopsy of tumour tissue is invasive, may be practically difficult, has resource implications and is clearly confounded by intratumoral heterogeneity. These shortcomings give huge potential to the recent advances in molecular imaging, which have the ability to visualize and quantify heterogeneity of tumour receptor expression, metabolism, apoptosis, blood flow or structure, non-invasively over time, *i.e.* at baseline and to assess response to treatment.

Owing to space constraints, we can only select a subset of imaging techniques for illustration purposes; a more comprehensive précis of the different image modalities has been reviewed elsewhere.[8]

VARIOUS IMAGING MODALITIES AND METHODS THAT CAN HELP TO MAP THE HETEROGENEITY IN TUMOUR METASTASIS

The development of metastasis is multifactorial and is dependent on the complex interaction between host factors and the tumour biology. This process is highly selective, and the metastatic lesion represents the end point of many sequential events that only a few cells can survive. Recent advances in next generation sequencing (NGS) have increased the understanding of (1) the clonal heterogeneity between primary and metastatic tumours and (2) the degree of genetic heterogeneity of metastatic tumours. For example, a study comparing sequences of primary tumours and metastases in lobular breast cancers revealed multiple mutations present only in metastases and several other mutations with increased frequency in metastatic sites.[9] Similarly, a number of studies report on the discordance in oestrogen receptor, progesterone receptor and human epidermal growth factor receptor 2 (HER2) expression between different metastatic sites.[10] As pointed out, histological analyses with repeated invasive biopsies have limitations. For instance, when different metastatic deposits are heterogeneous with respect to receptor expression and/or cellularity[11] and are not all subjected to biopsy, then a clinical decision based on *in vitro* analysis of the biopsied material may be prone to undersampling error. However, recent advances in imaging techniques, image acquisition and image analysis have been used to measure quantitative imaging biomarkers that may be able to address the complexities of tumour heterogeneity better than a standard histological biopsy. Here, we critically appraise these strategies specifically in the context of heterogeneous metastatic disease.

^{18}F-fludeoxyglucose–positron emission tomography/CT

Although CT is the imaging modality most widely used for tumour assessment, it provides very little in the way of distinct tumour activity information. The addition of positron emission tomography (PET) to CT can add such further information, and ^{18}F-fludeoxyglucose (^{18}F-FDG) is the most commonly used PET radiotracer, although there are many other radiotracers that examine different aspects of tumour biology. The ability of ^{18}F-FDG-PET to detect cancer is based on elevated aerobic glycolysis in the malignant tissue in comparison with the normal tissue—also known as the Warburg[12] effect. Although primarily reporting on tumour cell activity, ^{18}F-FDG-PET has been shown to also inform on tumour heterogeneity. A retrospective study using ^{18}F-FDG-PET/CT to monitor response among lesions in patients with bone-dominant metastatic breast cancer treated with systemic therapies reported that lesions showed heterogeneous metabolic response amongst responding and non-responding bony and non-bony lesions.[13]

Novel utilization of ^{18}F-FDG-PET/CT in recent years, such as texture analysis on CT imaging, has been shown to reflect tumour heterogeneity and associated prognosis. This has been examined in multiple tumour types, including lung,[14–16] colorectal[17–19] and oesophageal[20] cancers. There are a number of ways to extract texture elements in images. One such CT textural analysis methodology utilizes a two-step filtration–histogram technique. The first stage uses a Laplacian of gaussian spatial band-pass filter to selectively extract and enhance features of different sizes corresponding to fine, medium and coarse texture scales, allowing detection of spatial differences within a tissue (arising from the different band of spatial frequencies employed). The Laplacian detects intensity changes (or edges) within an image, which have been first smoothened by the gaussian distribution, based on the spatial scale filter (SSF) value. A lower SSF value (*e.g.* 2 mm) extracts and enhances features of a "finer" texture scale, whereas an

SSF value of 3, 4 or 5 mm extracts and enhances features of a "medium" texture scale and a higher SSF value (*e.g.* 6 mm) extracts and enhances features of a "coarser" texture scale, as shown in Figures 1 and 2. These novel texture analyses have also been applied to other imaging modalities, *e.g.* MRI,[21,22] and will be discussed later (section on Simultaneous positron emission tomography/MR and textural analysis).

Generation of these texture parameters provides vital information on the image features themselves (reviewed in Miles et al[23]). Standard deviation (SD) increases approximately in proportion to the square root of the number of features highlighted and their mean intensity difference compared with background (*i.e.* dark and bright features are both positive). Skewness is related to the average brightness of the highlighted features (predominantly bright features give positive values, while predominantly dark objects give negative values), which tends to zero with increasing number of features highlighted and moves away from zero with intensity variation in highlighted features. Kurtosis is related inversely to the number of features highlighted (whether bright or dark) and increases by intensity variations in highlighted features. By quantifying these different image features (size, concentration and density variation of the features highlighted by the filter) within a lesion (representing the different aspects of tissue heterogeneity), computed image texture analysis algorithms have the potential to provide additional morphological information relating to tumour heterogeneity. The intratumoral variability assessed by this technique is at a scale where the measured heterogeneity is likely to reflect tumour *vs* stroma and/or tumour *vs* necrosis. These features could feasibly correlate with a metastatic phenotype, but more work is required in this area to understand the associations between tumour–stromal relationships and gene expression and/or metastatic potential (see section Molecular imaging of metastatic potential). Yet, the prognostic application of CT textural analysis has been validated in various tumours types, with coarser tumours pertaining to a poorer prognosis[24] (Figure 3). In fact, overall survival (OS), progression-free survival (PFS) and local progression-free survival were all lower in individuals with high primary tumour coarseness.[25] Analysis of tumour texture in pre- and post-chemotherapy treatment in colorectal patients, to examine response and prognosis, has revealed that tumours that respond to treatment have lower initial tumour coarseness.[18] In addition to its correlation with survival, there is also limited pre-clinical literature which suggests that the application of these texture techniques can

Figure 1. (a) Conventional hepatic CT image. (b–d) Corresponding images selectively display (b) fine, (c) medium and (d) coarse texture obtained by using values for image filtration [spatial scale filter value (or sigma)] of 0.5 [width, 2 pixels (1.68 mm)], 1.5 [width, 6 pixels (5.04 mm)] and 2.5 [width, 12 pixels (10.08 mm)], respectively. Images should be viewed in the online format. Reproduced from Miles et al[18] with permission from the Radiological Society of North America.

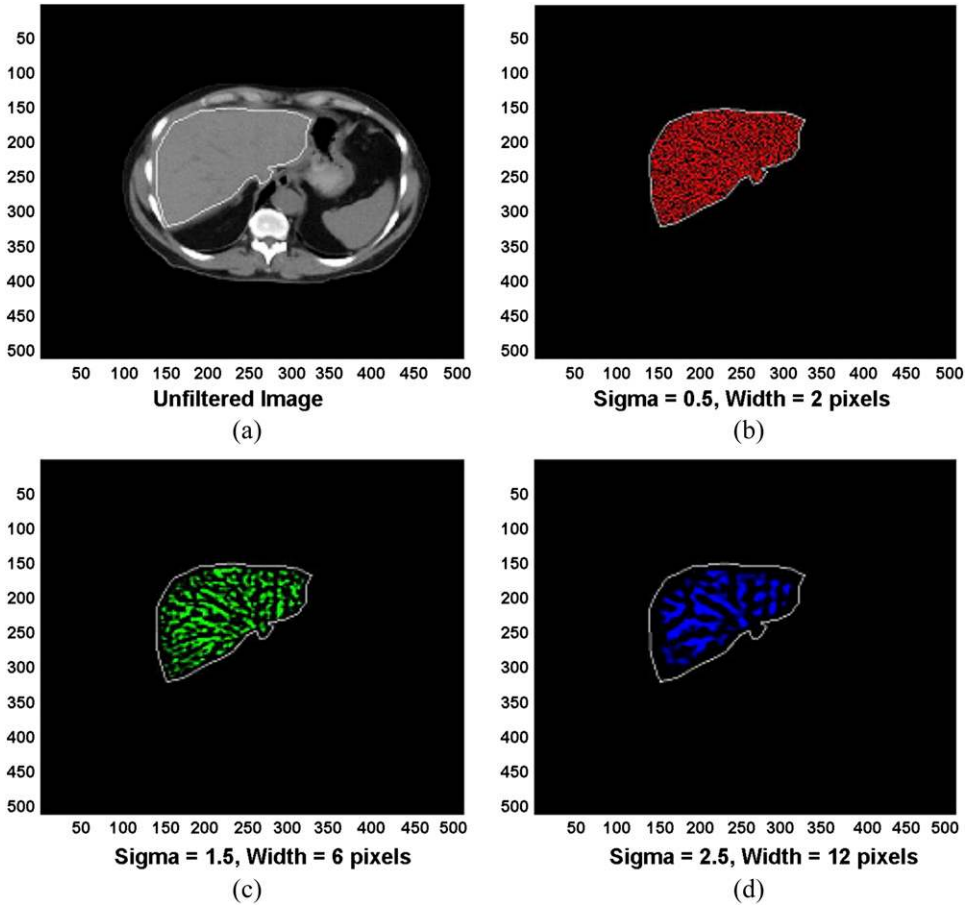

Figure 2. (a) A conventional CT (from a positron emission tomography/CT) image of a patient with a lung lesion and (b–d) corresponding images selectively displaying fine, medium and coarse texture obtained from TexRAD CT texture analysis (image heterogeneity) commercial research software (www.texrad.com, Radstock, UK). Images should be viewed in the online format.

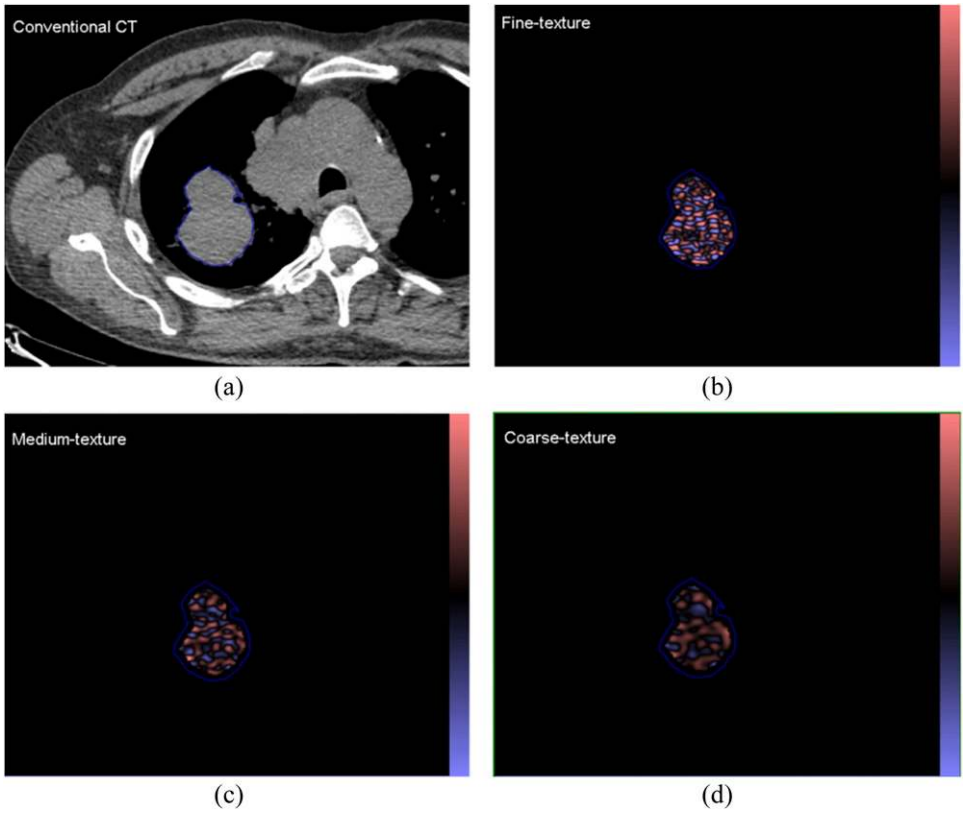

be used to analyse the surface heterogeneity of the primary tumour, and may yield non-invasive image parameters that may distinguish between metastatic and non-metastatic tumour phenotypes,[26] with exciting translational potential which needs further investigation.

PET texture analysis (PTA) can be conducted on the standardized uptake value (SUV) images used to measure the maximum SUV. The SUV images (individual pixel values) with initial units of uptake in Bq ml^{-1} can be converted (scaled) to SUV calibrated by patient weight and actual tracer activity (taking into consideration the initial tracer activity, amount of decay between the tracer measured time and scan time with respect to the half-life period of ^{18}F-FDG) with final units of uptake in g ml^{-1}. The tumour heterogeneity can be measured only on the SUV image without image filtration, using the histogram characteristics as described above in the section ^{18}F-fludeoxyglucose–positron emission tomography/CT. Image filtration is not appropriate owing to the inherently poor resolution of PET (SUV) data. A recent study in non-small-cell lung cancer (NSCLC) using PET/CT image data sets has shown the ability of PTA to be a prognostic marker of survival.[27] Other groups have shown that intra-tumour heterogeneity on PET via texture analysis predicts response to radiochemotherapy in oesophageal cancer (entropy, size, local and global heterogeneity and homogeneity, SUV),[28] and lung cancer (coarseness, contrast, busyness, complexity).[25] Given the poorer spatial resolution of PET compared with CT, the biophysical basis of metabolic textural features is not intuitive and requires further exploration.

Non-^{18}F-fludeoxyglucose–positron emission tomography for imaging the metastatic potential of primary tumours and/or detecting tumour metastases

^{18}F-fluoro-3′-deoxy-3′-L-fluorothymidine–positron emission tomography

^{18}F-fluorothymidine (FLT) is a tracer used to examine cell proliferation. Pyrimidine analogue thymidine is incorporated in DNA, during the S phase of the cell cycle, where proliferating cells synthesize DNA. ^{18}F-FLT is taken up by the cell and is phosphorylated by thymidine kinase 1. Thymidine kinase 1 activity is the highest during the cell division process in cells and takes place at a greater rate in malignant cells.[29] Given the dependence of this radiotracer on thymidine kinase 1 activity, there can be issues when used in conjunction with certain cytotoxic drugs, which arrest cells in S phase,[30] such as 5-fluorouracil. Various studies have been carried out on correlating imaging with histological findings and on immunostaining with Ki-67 to assess tumour proliferation rate. These studies have shown good correlation between the histological tumour proliferation rate and the ^{18}F-FLT-PET image.[31] Although ^{18}F-FLT-PET is an excellent tool for measuring tumour proliferation, there are several theoretical limitations to its use in detecting micrometastatic disease in patients with cancer. While an increase in proliferation is important for the initiation and maintenance of primary tumours, growth inhibition could ultimately be crucial for survival of carcinoma cells in the circulation. Mechanistically, this apparent paradox is

Figure 3. Kaplan–Meier plots demonstrating differences in patients with high and low primary tumour ^{18}F-fludeoxyglucose–positron emission tomography coarseness (a–c), contrast (d–f) and busyness (g–i). Differences in overall survival (OS) (a, d and g), progression-free survival (PFS) (b, e and h) and local progression-free survival (LPFS) (c, f and i) are demonstrated. Cum, cumulative. Reproduced from Cook et al[25] with permission from SN Turiel & Associates, Inc. © by the Society of Nuclear Medicine and Molecular Imaging, Inc.

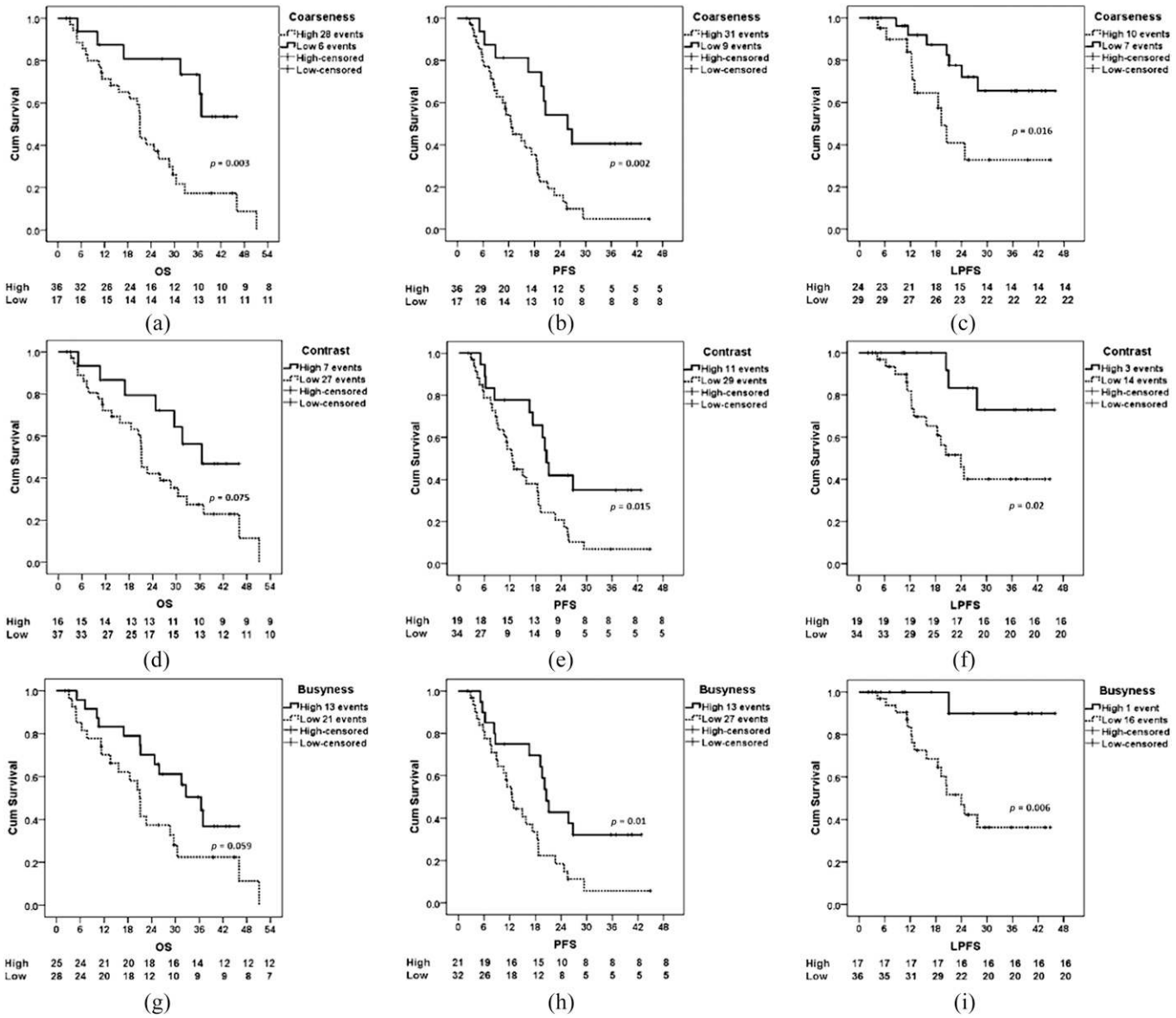

because of the dual function of cell cycle regulators, such as the well-known tumour suppressor gene p53[32] and transcription factor YB-1,[33] which also impact on the cell motility machinery. Additionally, metastatic cells in the target organ can enter into dormancy (*i.e.* a lag in tumour growth),[34] thus the sensitivity of detecting tumour metastases is somewhat limited.[35,36]

^{11}C-choline and ^{18}F-fluorocholine–positron emission tomography

Some tumours have low glucose metabolism, and therefore standard FDG-PET imaging has difficulties in the assessment of disease and treatment response. In prostate cancers, choline-PET imaging has been especially useful for restaging. Choline- and fluorocholine-based tracers used in PET scanning utilize the principle that choline is an essential component of the phospholipid portion of the cell membrane. It is particularly of benefit in a selected group of individuals rather than as a staging method for all; namely, patients with minimal recurrent prostate-specific antigen (PSA) levels of $\geq$1 ng ml^{-1}, those with short PSA doubling time (less than 3 months to a maximum of 6 months), and those with initial high recurrence risk tumour stage.[37,38]

Simultaneous positron emission tomography/MR

As discussed earlier in this review, PET image analysis traditionally focuses on the region of interest. The addition of MR to PET imaging can further add heterogeneity information regarding the

Figure 4. Produced from an imaging unit at the Institute of Nuclear Medicine, University College London, UK. Simultaneous ^{18}F-fludeoxyglucose–positron emission tomography (PET)/MRI-acquired image of a patient with a sigmoid tumour. Fused axial T_2 and PET (a), PET alone (b), MRI apparent diffusion coefficient map (c) and representative subtracted image from a dynamic contrast-enhanced MRI series (d); showing increased metabolism, cellularity and vascularity. Images should be viewed in the online format.

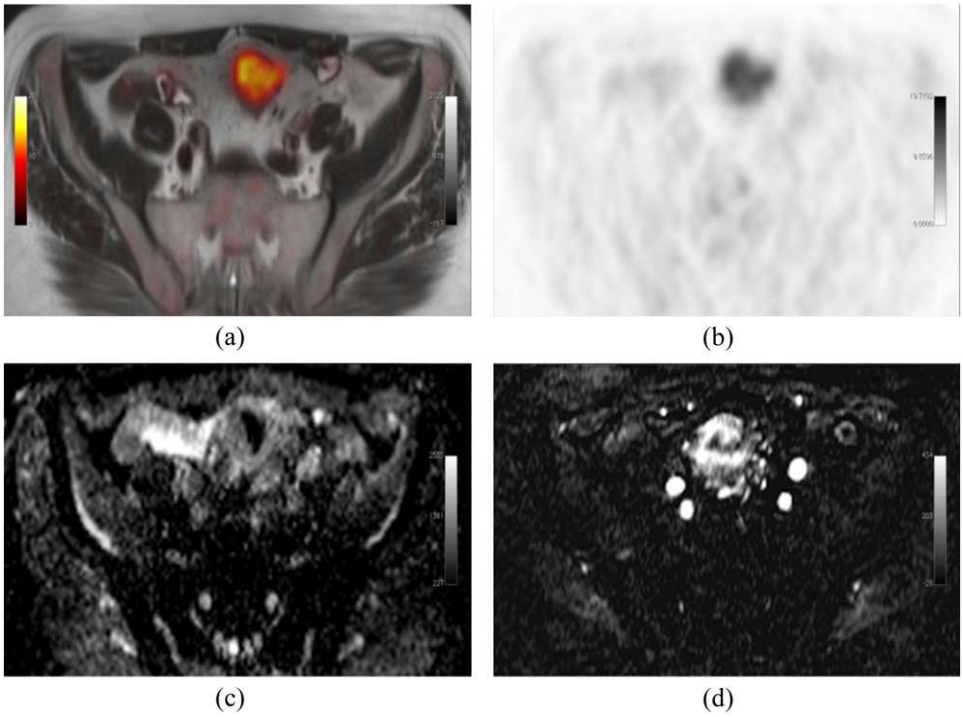

tumour phenotype that is gathered from radionuclide-based studies.[39] Dynamic contrast-enhanced (DCE) imaging differs from traditional MRI through the ability to acquire multiple images, before, during and after contrast injection (Figure 4). In the context of PET/MR, this imaging technique allows dynamic imaging of tumours to take place, with detailed imaging of tumour vascularity[40] through the concomitant evaluation of $\alpha_v\beta_3$ expression and high glucose metabolism within tumours that can show perfusion heterogeneity.[41] This form of imaging has also played a role in treatment assessment with vascular endothelial growth factor (VEGF) inhibitor use, which we discuss later on in further detail in this review (see section Molecular imaging of metastatic potential).

Ongoing developments in the combination of PET/MR with nanoparticle imaging have had further implications in the assessment of tumour heterogeneity.[42] Given the above discussion on specific (FDG- and non-FDG-based) PET tracers that are potentially of use in mapping the heterogeneity of different tumour types, the combination of specific-tracer PET/MR holds particular interest in imaging molecular heterogeneity.

The combination of microstructural and vascular information afforded by MRI with specific metabolic PET tracers can now be achieved in a clinic with whole-body PET/MR scanners.[43] Multiparametric imaging has well-recognized utility for microstructural and vascular tissue characterization and is rapidly establishing an expanding niche in the localization and management of prostate cancer.[44,45] Yet, in general, it remains more difficult to assess metabolic activity with MRI than with PET; MR spectroscopy (MRS) is inconsistently used in clinics, as it requires significant expertise in acquisition and processing of the MR signal; whilst hyperpolarized (HP) MRI in addition requires significant investment in infrastructure. Studies validating the use of whole-body PET/MR compared with PET/CT have repeatedly shown increased sensitivity in early tumour detection, and using diffusion weighting on top of PET/MR can also detect treatment response at varying levels within metastases.[46–50]

Multiparametric PET/MR performed by our group demonstrates the ability to assess glycolysis, cellularity and water content and intralesional heterogeneity (via texture analysis) within a single examination (Figure 5). In general, we found that tumours with more heterogeneous water distribution (*i.e.* higher SD and proportion of positive pixels) were more cellular (*i.e.* lower mean apparent diffusion coefficient) and glycolytic (*i.e.* higher SUV_{mean}). Foci of high cellularity also correspond to areas of increased glycolysis. Textural filters applied to the fractional water images revealed features of around 3- to 4-mm bright objects, which may be associated with pockets of water content and tended to be higher within tumours having adverse biology (restricted diffusion and increased glucose uptake). Multiparametric PET/MRI data sets evaluating tissue microstructure, metabolism and heterogeneity are likely to contain prognostic information/relate to metastatic potential; both hypotheses require further work to validate.

Furthermore, simultaneous PET/MRI offers the opportunity in the clinic to combine tissue characterization multiparametric

Figure 5. Multiparametric positron emission tomography (PET)/MRI of a rectal cancer. (a) High ^{18}F-fludeoxyglucose uptake on fused PET/T_2 MRI, with (b) a correspondingly patchy reduced apparent diffusion coefficient (ADC) in keeping with pockets of high cellularity within the tumour and (c) a fractional water image derived from source fat and water Dixon images of the same tumour confirms that areas of increased cellularity correlate with relatively increased water content (white arrows). (d) Application of a medium coarse textural filter highlights 3- to 4-mm bright objects on the fractional water image (medium texture map). Images should be viewed in the online format. (www.texrad.com, Radstock, UK.)

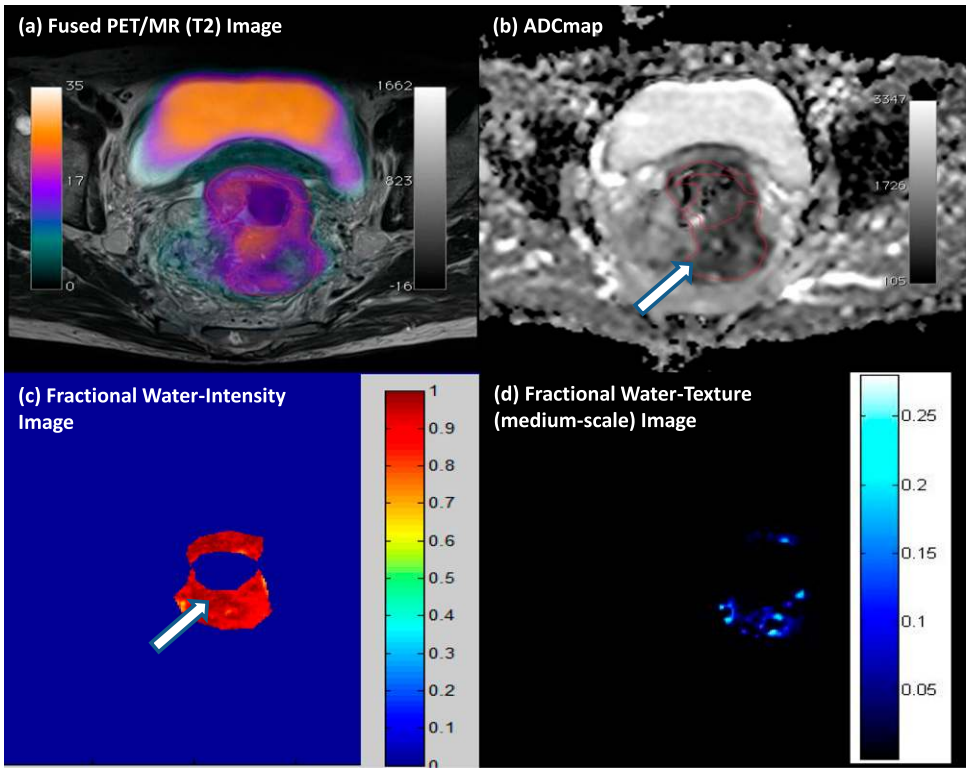

MRI with specific molecular PET imaging, with the potential to assess dynamic biological relationships through multimodal imaging of, for example, tumour cellularity/cell turnover [diffusion-weighted imaging (DWI) or FLT-PET], hypoxia (blood oxygen level-dependent MRI or ^{18}F-fluoromisonidazole PET ligand), vascularity (DCE/MRI or α-V-β-3 PET ligand) and glycolysis (^{18}F-FDG-PET ligand or glucose chemical exchange saturation transfer MRI).[51] Spatial heterogeneity of PET-MRI signals among metastases is often evident.[11] Elucidating the mechanisms leading to heterogeneous multimodal metastatic phenotypes and the consequent therapeutic implications remains the remit of future research.

Imaging the link between metabolism and tumour signalling pathways that are associated with metastasis: hyperpolarized MRI

^{13}C-MRS has been used in the investigation of metabolic processes *in vivo* for many years.[52] Its limitations relate to the difficulty in the signal intensity of the proteins in question, mainly down to the physics of MRI and its use of the apparent diffusion coefficient of water. Hyperpolarization with the dynamic nuclear polarization technique can yield >10 000-fold signal increases in MR-active nuclei, allowing the detection of ^{13}C-labelled substrates *in vivo* and also imaging of tissue distribution, in the absence of any background signal from non-polarized material. Pyruvate is a molecule involved in major metabolic and catabolic pathways in mammalian cells (Krebs cycle) and depending on anaerobic or aerobic metabolism can have various end products. 1-^{13}C-pyruvate imaging can therefore detect lactate, alanine and carbon dioxide.[53,54] The imaging data generated by this technique in a transgenic mouse model of prostate adenocarcinoma were shown to correlate with the histological grading of tumours and have been used to identify tumour necrosis and metastatic lymph nodes. The NCT01229618 clinical trial is examining the role of 1-^{13}C-pyruvate imaging in patients with prostate cancer.[55] HP ^{13}C MR spectroscopic imaging, measuring the HP lactate-to-pyruvate ratios, can be used to monitor the heterogeneity in a major signalling pathway within cancers, namely the PI3K/AKT/mTOR pathway and its response to molecule-targeted therapeutics, such as Everolimus,[56] and potentially inhibitors of other signalling pathways, *e.g.* hypoxia-inducible factor-1 and MYC, which are known to predispose tumour cells to metastasize under both normoxic and hypoxic conditions.[57–59]

Nanoparticle-based imaging

Nanoparticles are small, 1–100 nm, structures that in recent years have been explored in their capacity for imaging, drug delivery and monitoring of treatment outcome.[60] Nanoparticles may be organic based (liposomes, polymeric nanoparticles, micelles, dendrimers and solid lipid nanoparticles), inorganic based (iron oxide

nanoparticles, gold nanoparticles, semiconductor nanocrystals, ceramic nanoparticles and carbon nanotubes) or a hybrid of both. Nanoparticles have large surface to volume ratios contributing to their high loading capacity. As drug delivery systems, nanoparticles have been shown to improve drug solubility, prolong blood circulation half-life and control drug release.[61] One of the major advantages with nanoparticle technology is that drug delivery and imaging probes can be combined into one delivery system.

Gold nanoparticles have high density and extinction coefficients and can be applied as contrast agents for CT, dark field imaging and photoacoustic imaging. The shape of gold nanoparticles can facilitate them to strongly absorb light in the near-infrared range, converting this energy into heat for photothermal therapy. Iron oxide-based nanoparticles are magnetic and therefore used as contrast agents to produce hypodense regions on T_2/T_2 weighted MR images.

Nanoparticles have also been used as a predictive tool in functional imaging. Superparamagnetic iron oxide nanoparticles (SPIONs), specifically reporting on tumour vasculature, have recently been used in predicting the likelihood of brain metastases in melanomas.[62,63] Various imaging nanoparticles are currently undergoing human clinical trials; for example, ^{124}I-labelled cRGDY silica nanoparticles in melanoma (NCT01266096), ^{99m}TC-sulphur colloid nanoparticles in sentinel node mapping in breast cancers (NCT00438477) and ultrasmall (U)SPION in pre-operative pancreatic cancers (NCT00920023). All of the above are a mixture of imaging modalities, CT, MRI and single photon emission CT (SPECT), showing that nanoparticle imaging is not exclusive to one imaging modality. A specific application of these (U)SPIOs to characterize the heterogeneity of macrophage infiltration in the tumour microenvironment will be described in section Application of an integrated imaging–genomic approach to stratify cancer treatment—requirements for clinical translation.

Imaging tumour heterogeneity at a cellular level: intra-operative optical imaging

The basis of radio-guided surgery involves the deployment of a radiolabelled tumour tracer pre-operatively and the use of a detection probe intra-operatively. Intra-operative use of a gamma probe has been shown to reveal small (<10 mm) lesions within the abdomen that can be missed on traditional whole-body functional imaging. This technique has been shown to individualize surgical procedures intra-operatively, resulting in improved complete resection rates with subsequent effects on reducing recurrence rates.[64–67] Moreover, to facilitate the visualization of cancer cells at a higher resolution, intra-operative tumour imaging has been successfully conducted with near-infrared dye-labelled molecule-targeted antibodies against various tumour cell targets, *e.g.* folate receptor, VEGF (bevacizumab) and HER2 (trastuzumab).[68,69] The first-in-man ovarian cancer surgery was performed with an optical detection device that has a corresponding resolution varying between 150 and 30 μm.[69] It allows for individual cellular clusters to be visualized and dissected. Further genomic investigations of these cellular clusters is likely to add further details to the degree of cell-to-cell tumour heterogeneity and its role in promoting resistance within an evolving tumour genome.

MOLECULAR IMAGING OF METASTATIC POTENTIAL

Early identification of patients at high risk of metastatic disease is arguably the most important task for improving cancer mortality. The pre-metastatic niche hypothesis comprises the creation of a supportive environment for circulating tumour cells to "seed" to.[70] This dynamic process is thought to involve both chemokine secretion at the primary tumour site and subsequent activation of immune cells in the target tissue of metastasis. In response to tumour-secreted factors (TSFs), intra- and extramedullary haematopoiesis and consecutive immune cell differentiations are altered in order to promote the survival and outgrowth of disseminated tumour cells. Certain organs carry a greater susceptibility to specific tumours; for example, bone metastases are prevalent in breast and prostate cancers, whereas are rarer in others, such as ovarian. The understanding of tumour heterogeneity should allow us to not only assess the primary tumour at a molecular level but also examine distant organs for pre-metastatic changes.

Although targeted SPECT and PET probes mostly address surface markers or metabolic features of the primary tumour cells themselves, the same principles can be used for visualization of metastasis-associated changes of tissue composition or intercellular communication. Using a PET imaging probe for vascular cell adhesion molecule-1 (VLA-4), reportedly highly expressed in bone marrow-derived cells that have been implicated in establishing the pre-metastatic niche,[71] Shokeen et al[72] reported using imaging combined with immunohistochemistry, an enrichment of these haematopoietic progenitor cells (HPCs) at the sites of metastasis. Besides the HPCs, tumour-associated macrophage (TAM) accumulation in the tumour microenvironment has been linked to increased tumour invasiveness and therefore metastasis[5] In primary tumours, visualization of TAM by MRI is established and frequently performed using macromolecular substances that are taken up by the target cells via phagocytosis, such as (U)SPIONs,[73] as mentioned earlier in this review. Nevertheless, the limited sensitivity of MRI (compared with the extremely high sensitivity of PET microdosing), combined with the high background activity of phagocytic cells in typical target organs of metastasis, would, however, probably hinder the use of such techniques in imaging of pre-metastatic tissue priming.

Another aspect of the promoting effect of TAM on tumour metastasis is through enhanced angiogenesis, partly through an increase in VEGF secretion by macrophages.[74–77] VEGF is an important signalling pathway in vasculogenesis and angiogenesis, and therefore plays a vital role in tumour growth, survival and metastases. In oncology, there have been multiple anti-VEGF therapies, of various forms, monoclonal antibodies (bevacizumab) and small tyrosine kinase inhibitors (pazopanib). The use of DCE/MR in vascular imaging has already been discussed in the assessment of angiogenesis. The lack of an appropriate biomarker for VEGF inhibitors has been a particular issue in the clinical setting. VEGF inhibitors are used widely in various tumour types, such as breast,[78] colon,[79] ovarian,[80] renal cell[81] and hepatocellular;[82] however, treatment response can be very difficult to assess, especially in the maintenance setting. DCE/MRI allows non-invasive

quantification of tumour microvasculature through dynamic imaging of enhancement and washout of injected contrast material. The vascular configuration in tumours promotes an initial faster and greater accumulation of contrast within the interstitial space and favours more rapid removal of contrast from the interstitium, as the concentration of contrast in the blood falls owing to renal excretion. These features can be fitted to pharmacokinetic models, and the derived variables have been directly related to VEGF modulation of vascular permeability.[83,84]

Imaging of mediators of inflammation, such as tumour necrosis factors or interleukin-1α, has been performed successfully in clinical and experimental imaging of inflammation.[85,86] However, given the high background activity and relatively low specific accumulation of the respective tracers at the target site where there is a significant degree of inflammation, it is not hopeful that the subtle potential changes in pre-metastatic tissue could specifically be picked up using these or comparable approaches. It has recently been established that, in pre-metastatic lung tissue of tumour-bearing animals, the vessel permeability is locally altered in response to TSFs,[87] resembling local inflammation. This permeability as well as the accompanied increase in extravascular cellularity (*e.g.* inflammatory cell content in the extravascular compartment) could in theory be visualized using established imaging approaches such as MRI.[88,89] It would be of interest to see changes in tissue architecture and other MRI-based assessment of features, such as collagen content, consecutive mechanical characteristics, vessel architecture etc., that are revealed during the establishment of metastasis.

Moreover, further investigation of the cellular composition of the pre-metastatic niche and the main regulating factors is strongly required.[90] It would potentially enable the use of specific MRI approaches for tissue characterization as well as an armament of specific probes for radionuclide and optical imaging of already established disease-associated target molecules and cells.[91] In this context, exosomes are 40- to 100-nm-diameter membrane vesicles of endocytic origin that have been demonstrated to contain mRNA, miRNA and proteins, and are gaining increasing interest in terms of their translational research potential in cancer.[92–96] They are released into the extracellular space from various cell types and body fluids and mediate intercellular transfer of RNAs and proteins. As such, exosome analysis is ideally suited for monitoring the evolving tumour longitudinally, in terms of its whole transcriptome, miRNome and proteome profiles.[92,97] Exosomes have been shown to have an important role in intercellular communication, and they are involved in stimulation of the secretion of growth factors, cytokines. There is growing evidence that exosomes are generally involved in the manipulation of the pre-metastatic niche.[96,98,99] Imaging the transfer of exosomes secreted by tumour cells into host cells in a cancer mouse model suggests that the tumour-derived exosomes contribute to the formation of a niche to promote tumour growth and metastasis.[100] A number of current studies have shown that there is a correlation between exosomes and metastasis in different types of cancers. The detection and quantification of exosomes carrying tumour-relative antigens in melanoma patients may represent a potential tool for cancer screening and prediction of metastatic risk.[101] Tumour-derived microvesicles from patients with head and neck cancer induce apoptosis of activated $CD8^+$ T cells that correlated with disease activity and the presence of lymph node metastases.[102] Furthermore, exosomes adapt to hypoxia in the local tumour microenvironment during cancer progression and thus reflect the hypoxic state of cancer cells. Under hypoxic conditions, a change of the protein cargo of exosomes secreted by tumour cells was observed that modulates the microenvironment and promotes angiogenesis and metastasis.[95] In highly aggressive brain tumours, the analysis of exosomes from patient samples reveals the enrichment in exosomes of hypoxia-regulated mRNAs and proteins.[103] In addition to the *in vitro* analysis of plasma/serum exosomes, the effect of the exosomes on pulmonary vascular permeability[96] can be assessed by the aforementioned MR-based whole-body imaging techniques.

Clinically, exosomes are increasing in prominence for their diagnostic/predictive potential in cancers. For example, the tumour suppressor gene phosphatase and tensin homolog is only expressed in exosomes that circulate in the blood of patients with prostate cancer, but it is not detected in exosomes from normal subjects, and might be thus a potential biomarker for prostate cancer.[104] In another study, potential diagnostic markers for human NSCLC were identified by proteomic analysis of purified microvesicles from pleural effusion in patients with NSCLC.[102] Micro-RNA and protein profiling of brain metastasis cell-derived exosomes *vs* non-brain metastasis revealed changes in specific miRNA and proteins which may contribute to the discovery of new biomarkers for brain metastasis.[105] Similarly, proteome profiling of exosomes from human primary and metastatic colorectal cancer reveal different expression of key metastatic factors.[106] These examples demonstrate the increasing importance of exosomes in the identification of

Figure 6. Intertumour heterogeneity of gene expression profiles associated with cellular processes and disease progression. Unsupervised hierarchical clustering showing pair-wise correlations of a panel of gene signature scores across primary breast tumour tissue samples (234 patients). Representative signatures are indicated for each cluster: T-cells, B-cells and dendritic cells, Immune1*, Motility, stem-cell-like, tumour growth factor β (TGFβ) response, RAS*, Stroma2*, GGI*, Gene70*, MYC* (*signature curated by Ignatiadis et al[112]). Recent studies report expression-based prognostic and predictive stratification of primary breast tumours, which are phenotypically similar according to current clinical methods.[111,113,114] Images should be viewed in the online format.

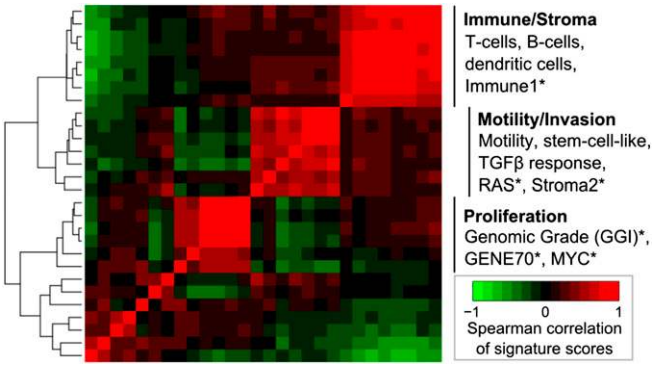

Figure 7. Schematic of potential future trial design, incorporating functional imaging and tissue samples to further biomarker research.

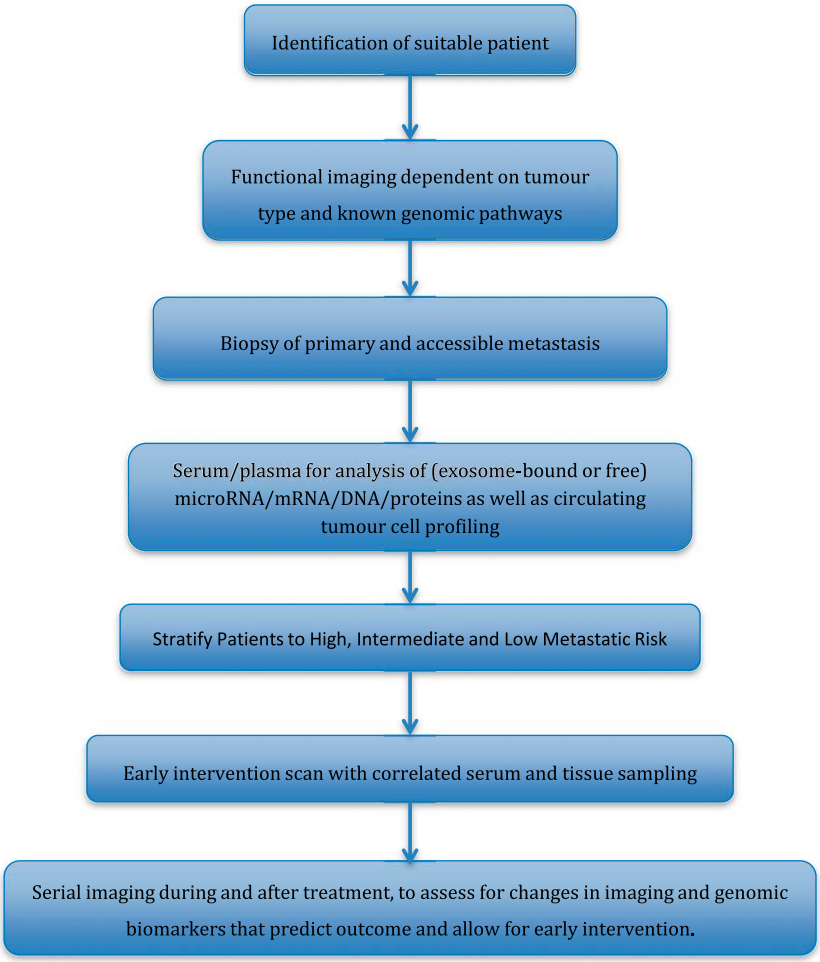

novel biomarkers in metastatic cancers, although imaging in patients is still a little way off clinical application.[107]

APPLICATION OF AN INTEGRATED IMAGING–GENOMIC APPROACH TO STRATIFY CANCER TREATMENT—REQUIREMENTS FOR CLINICAL TRANSLATION

Much energy has been expended recently in establishing the role of imaging biomarkers for evaluating treatment response in cancers. An ongoing collaborative effort by the American College of Radiology Imaging Network (ACRIN), Philadelphia, PA, Cancer and Leukaemia Group B, Chicago, IL, and the National Cancer Institute, Bethesda, MD, Specialized Programs of Research Excellence recently conducted the largest multicentre imaging trial (ACRIN 6657) as part of the I-SPY1 trial (Investigation of Serial Studies to Predict Your Therapeutic Response With Imaging and Molecular Analysis). ACRIN 6657 utilizes MRI to measure treatment response in patients receiving neoadjuvant chemotherapy.[108] Volumetric estimates of the tumour size, based on functional criteria applied to contrast-enhanced images, were seen to have greater sensitivity than linear tumour diameter measurements for predicting pathologically complete responses in patients completing neoadjuvant chemotherapy. The greatest difference in predictive ability occurred at the early time points, providing "proof of concept" that imaging parameters can serve as non-invasive predictive biomarkers of early treatment response. Its subsequent I-SPY2 clinical trial platform targeting the rapid focused clinical development of paired oncologic therapies and biomarkers now uses MR volumes to provide information about response to chemotherapy between regimens—information that cannot otherwise be obtained without surgical resection.[109] Additionally, its sub-study, ACRIN 6698, combines both DCE and DWI MRI data to generate novel imaging biomarkers that may correlate with treatment response,[110] and its results are eagerly awaited. Integration of these imaging biomarkers with genomic profiles of tumours are likely to prove essential for future clinical translation.

Transcriptomic analyses of primary solid tumours have revealed differential activation of gene expression signatures relating to cellular processes, including proliferation, cell migration and immune response (Figure 6) with the potential for prognostic and predictive stratification of tumours, which are phenotypically similar by current clinical methods.[111,112,115] Meanwhile, putative associations between clinical imaging traits and gene expression profiles have been reported in solid tumours. Exploratory studies have reported correlations between selected image traits and the

expression of individual genes or larger modules of co-expressed genes[113,116] reviewed in Rutman and Kuo.[117] Genomic copy number and other genomic aberrations exhibit variation between tumours from different patients[118,119] and between subclones within a primary tumour[4,120] Lesional and temporal variations in HER2 amplification and specific HER2 insertional mutations (such as $HER2^{YVMA}$), for example, could have clinical implications for HER2-targeted treatment and monitoring in the metastatic setting.[121,122] PET imaging using tracer-linked trastuzumab has been used to identify HER2-positive tumour and metastatic sites,[123,124] indicating the potential for non-invasive monitoring of HER2-positive lesions. In the treatment–response setting, early metabolic response to trastuzumab (less than 48 h post treatment) was detected in a pre-clinical study using optical metabolic imaging but not FDG-PET.[125] Many more genomic aberrations have been catalogued as part of large-cohort studies of primary solid tumours, revealing both recurrent mutations (*e.g.* p53, PIK3CA[119,126]) and recurrent dysregulation associated with a diversity of less frequent underlying genomic or transcriptional variation.[121,127] Detection of intertumoral, interlesional and temporal variations may prove to be critical for describing and monitoring disease progression but would require methods for non-invasive detection. Non-invasive imaging, coupled to more advanced analyses, may in the future yield parameters that oncologists can monitor longitudinally, in conjunction with high-coverage NGS of plasma-derived DNA to monitor the evolution of tumour genomic profiles under treatment pressure.[128] Some initial results have shown that there may be a correlation between some of these mutations (codons 12, 13 and 61 of KRAS, for instance) and various PET/CT-based parameters in colorectal cancers.[129]

TRANSLATION OF IMAGING TECHNOLOGIES IN ONCOLOGICAL TRIALS

Given the lack of measurable biomarkers through patient sampling, the advances in molecular imaging provide an impetus for testing functional imaging as a cancer biomarker, in a way that is complementary to tissue- and blood-based biomarkers. Despite these rapid advances, the translation of such techniques into clinics continues to lag behind. Incorporation of functional imaging to evaluate tumour responses should play an important role in designing future trials (Figure 7). Strategically planned biomarker evaluations with access to functional imaging in early phase trials (Phase I/II) will allow for efficient Phase III clinical trial designs, increasing the chances of positive Phase III biomarker-driven trial results. Functional imaging can not only provide information on the treatment response but can also monitor mutational pathways and the various molecular pathway pressures on an individual tumour, allowing a more robust stratification of treatment pathways. A major setback for targeted therapy has been the duration of tumour response, as many patients go on to have progressive disease after a relatively short response period. At present, although we understand a small fraction of these tumour escape pathways, we are unable to respond in a clinical setting to early mutational changes. Functional imaging information can help identify and assess high-/at-risk patients non-invasively, allowing for implementation of appropriate management plans governed by their personal escape pathway and thereby improving patient outcome.

At present robust large patient trials examining the methods we have discussed in this review are lacking. However, a few large trials are currently incorporating functional imaging within their remit. The NeoPHOEBE trial is a Phase II trial examining the application of FDG-PET as a biomarker of early response in the neoadjuvant setting in the treatment of HER2-positive breast cancer. Similarly, the FOCUS4 trial, currently recruiting, is a molecularly stratified randomized trial for patients with inoperable or metastatic colorectal cancer. It contains five arms [v-raf murine sarcoma viral oncogene homolog B (BRAF), PI3KCA, RAS, no mutation and non-classified] of randomization with prior histological analysis of patient pathology determining treatment. Despite the optimism behind these trials, the need for robust validation is crucial in order to offer patients lasting results.

The role of clinical trials should not be purely to review efficacy of treatment but also to aid the development of new research. To this end, the acquisition of patient samples at each step of the treatment paradigm plays a vital role in developing the translational application of research. As previously discussed, the role of exosomes in cancers is developing in prominence and understanding alongside the emerging role of circulating tumour cells and their reflection of the primary and metastatic tumour.

The integration of functional imaging, patient sampling and drug development together with wider research is likely to play a key role in fully understanding the nature of heterogeneity and ultimately how to control its effects to clinical advantage.

CONCLUSION

In this review, we have discussed the novel application of current imaging techniques in the assessment of heterogeneity especially in the context of examining metastasis and predicting metastatic potential. Although we have access to and are developing new tracers and new imaging techniques, there is a significant need for large patient trials and applications to fully determine their specific validity in the personalized patient treatment paradigm.

CONFLICTS OF INTEREST

B. Ganeshan and K.A. Miles are shareholders in TexRAD Ltd, a company developing and marketing the commercial (research) texture analysis software.

FUNDING

This work was supported by KCL Breakthrough Breast Cancer Research Unit/Sarah Green Fellowship funding (SI) and an endowment fund from Dimbleby Cancer Care to King's College London (TN). KL and ME were supported by the KCL-UCL Comprehensive Cancer Imaging Centre funding [CR-UK & EPSRC, in association with the MRC and DoH (England)]. HM was supported by an FP7-HEALTH-2010 European Union grant entitled "IMAGINT" (grant no. 259881). This work was undertaken at UCLH/UCL, which received a proportion of the funding from the UK's Department of Health's NIHR Biomedical Research Centre's funding scheme. Further funding was received from other NIHR sources.

REFERENCES

1. Fruhwirth GO, Fernandes LP, Weitsman G, Patel G, Kelleher M, Lawler K, et al. How Förster resonance energy transfer imaging improves the understanding of protein interaction networks in cancer biology. *Chemphyschem* 2011; **12**: 442–61.
2. Virchow R. *Die cellular pathologie in ihrer begründung auf physiologische und pathologische gewebelehre*. Berlin, Germany: August Hirschwald; 1858.
3. Navin N, Kendall J, Troge J, Andrews P, Rodgers L, McIndoo J, et al. Tumour evolution inferred by single-cell sequencing. *Nature* 2011; **472**: 90–4. doi: 10.1038/nature09807
4. Gerlinger M, Rowan AJ, Horswell S, Larkin J, Endesfelder D, Gronroos E, et al. Intratumor heterogeneity and branched evolution revealed by multiregion sequencing. *N Engl J Med* 2012; **366**: 883–92. doi: 10.1056/NEJMoa1113205
5. Quail DF, Joyce JA. Microenvironmental regulation of tumor progression and metastasis. *Nat Med* 2013; **19**: 1423–37.
6. Psaila B, Lyden D. The metastatic niche: adapting the foreign soil. *Nat Rev Cancer* 2009; **9**: 285–93.
7. Hüsemann Y, Geigl JB, Schubert F, Musiani P, Meyer M, Burghart E, et al. Systemic spread is an early step in breast cancer. *Cancer Cell* 2008; **13**: 58–68.
8. Patel GS, Kiuchi T, Lawler K, Ofo E, Fruhwirth GO, Kelleher M, et al. The challenges of integrating molecular imaging into the optimization of cancer therapy. *Integr Biol (Camb)* 2011; **3**: 603–31. doi: 10.1039/c0ib00131g
9. Shah SP, Morin RD, Khattra J, Prentice L, Pugh T, Burleigh A, et al. Mutational evolution in a lobular breast tumour profiled at single nucleotide resolution. *Nature* 2009; **461**: 809–13. doi: 10.1038/nature08489
10. Hoefnagel LD, van der Groep P, van de Vijver MJ, Boers JE, Wesseling P, Wesseling J, et al. Discordance in ERα, PR and HER2 receptor status across different distant breast cancer metastases within the same patient. *Ann Oncol* 2013; **24**: 3017–23.
11. Gaertner FC, Fürst S, Schwaiger M. PET/MR: a paradigm shift. *Cancer Imaging* 2013; **13**: 36–52.
12. Warburg O. On the origin of cancer cells. *Science* 1956; **123**: 309–14.
13. Huyge V, Garcia C, Alexiou J, Ameye L, Vanderlinden B, Lemort M, et al. Heterogeneity of metabolic response to systemic therapy in metastatic breast cancer patients. *Clin Oncol (R Coll Radiol)* 2010; **22**: 818–27. doi: 10.1016/j.clon.2010.05.021
14. Ganeshan B, Goh V, Mandeville HC, Ng QS, Hoskin PJ, Miles KA. Non–small cell lung cancer: histopathologic correlates for texture parameters at CT. *Radiology* 2013; **266**: 326–36.
15. Ganeshan B, Panayiotou E, Burnand K, Dizdarevic S, Miles K. Tumour heterogeneity in non-small cell lung carcinoma assessed by CT texture analysis: a potential marker of survival. *Eur Radiol* 2012; **22**: 796–802. doi: 10.1007/s00330-011-2319-8
16. Ganeshan B, Abaleke S, Young RCD, Chatwin CR, Miles KA. Texture analysis of non-small cell lung cancer on unenhanced computed tomography: initial evidence for a relationship with tumour glucose metabolism and stage. *Cancer Imaging* 2010; **10**: 137–43.
17. Ganeshan B, Miles KA, Young RCD, Chatwin CR. Hepatic enhancement in colorectal cancer: texture analysis correlates with hepatic hemodynamics and patient survival. *Acad Radiol* 2007; **14**: 1520–30. doi: 10.1016/j.acra.2007.06.028
18. Miles KA, Ganeshan B, Griffiths MR, Young RC, Chatwin CR. Colorectal cancer: texture analysis of portal phase hepatic CT images as a potential marker of survival. *Radiology* 2009; **250**: 444–52. doi: 10.1148/radiol.2502071879
19. Ganeshan B, Miles KA, Young RC, Chatwin CR. In search of biologic correlates for liver texture on portal-phase CT. *Acad Radiol* 2007; **14**: 1058–68. doi: 10.1016/j.acra.2007.05.023
20. Cheng NM, Dean Fang YH, Chang JT, Huang CG, Tsan DL, Ng SH, et al. Textural features of pretreatment 18F-FDG PET/CT images: prognostic significance in patients with advanced T-stage oropharyngeal squamous cell carcinoma. *J Nucl Med* 2013; **54**: 1703–9.
21. Brown R, Zlatescu M, Sijben A, Roldan G, Easaw J, Forsyth P, et al. The use of magnetic resonance imaging to noninvasively detect genetic signatures in oligodendroglioma. *Clin Cancer Res* 2008; **14**: 2357–62. doi: 10.1158/1078-0432.CCR-07-1964
22. Foroutan P, Kreahling JM, Morse DL, Grove O, Lloyd MC, Reed D, et al. Diffusion MRI and novel texture analysis in osteosarcoma xenotransplants predicts response to anti-checkpoint therapy. *PLoS One* 2013; **8**: e82875.
23. Miles KA, Ganeshan B, Hayball MP. CT texture analysis using the filtration-histogram method: what do the measurements mean? *Cancer Imaging* 2013; **13**: 400–6. doi: 10.1102/1470-7330.2013.9045
24. Ganeshan B, Skogen K, Pressney I, Coutroubis D, Miles K. Tumour heterogeneity in oesophageal cancer assessed by CT texture analysis: preliminary evidence of an association with tumour metabolism, stage, and survival. *Clin Radiol* 2012; **67**: 157–64.
25. Cook GJ, Yip C, Siddique M, Goh V, Chicklore S, Roy A, et al. Are pretreatment 18F-FDG PET tumor textural features in non-small cell lung cancer associated with response and survival after chemoradiotherapy? *J Nucl Med* 2013; **54**: 19–26. doi: 10.2967/jnumed.112.107375
26. Fan X, River JN, Zamora M, Tarlo K, Kellar K, Rinker-Schaeffer C, et al. Differentiation of nonmetastatic and metastatic rodent prostate tumors with high spectral and spatial resolution MRI. *Magn Reson Med* 2001; **45**: 1046–55.
27. Win T, Miles KA, Janes SM, Ganeshan B, Shastry M, Endozo R, et al. Tumor heterogeneity and permeability as measured on the CT component of PET/CT predict survival in patients with non-small cell lung cancer. *Clin Cancer Res* 2013; **19**: 3591–9. doi: 10.1158/1078-0432.CCR-12-1307
28. Tixier F, Hatt M, Le Rest CC, Le Pogam A, Corcos L, Visvikis D. Reproducibility of tumor uptake heterogeneity characterization through textural feature analysis in 18F-FDG PET. *J Nucl Med* 2012; **53**: 693–700.
29. Boothman DA, Davis TW, Sahijdak WM. Enhanced expression of thymidine kinase in human cells following ionizing radiation. *Int J Radiat Oncol Biol Phys* 1994; **30**: 391–8.
30. Mirjolet JF, Barberi-Heyob M, Merlin JL, Marchal S, Etienne MC, Milano G, et al. Thymidylate synthase expression and activity: relation to S-phase parameters and 5-fluorouracil sensitivity. *Br J Cancer* 1998; **78**: 62–8.
31. Francis DL, Freeman A, Visvikis D, Costa DC, Luthra SK, Novelli M, et al. In vivo imaging of cellular proliferation in colorectal cancer using positron emission tomography. *Gut* 2003; **52**: 1602–6.
32. Roger L, Gadea G, Roux P. Control of cell migration: a tumour suppressor function for p53? *Biol Cell* 2006; **98**: 141–52.

33. Evdokimova V, Tognon C, Ng T, Sorensen PH. Reduced proliferation and enhanced migration: two sides of the same coin? Molecular mechanisms of metastatic progression by YB-1. *Cell Cycle* 2009; **8**: 2901–6.
34. Giancotti FG. Mechanisms governing metastatic dormancy and reactivation. *Cell* 2013; **155**: 750–64.
35. Troost EGC, Vogel WV, Merkx MA, Slootweg PJ, Marres HA, Peeters WJ, et al. 18F-FLT PET does not discriminate between reactive and metastatic lymph nodes in primary head and neck cancer patients. *J Nucl Med* 2007; **48**: 726–35. doi: 10.2967/jnumed.106.037473
36. Troost EG, Bussink J, Oyen WJ, Kaanders JH. 18F-FDG and 18F-FLT do not discriminate between reactive and metastatic lymph nodes in oral cancer. *J Nucl Med* 2009; **50**: 490–1. doi: 10.2967/jnumed.108.055962
37. Umbehr MH, Müntener M, Hany T, Sulser T, Bachmann LM. The role of 11C-choline and 18F-fluorocholine positron emission tomography (PET) and PET/CT in prostate cancer: a systematic review and meta-analysis. *Eur Urol* 2013; **64**: 106–17. doi: 10.1016/j.eururo.2013.04.019
38. Yang Z, Sun Y, Zhang Y, Xue J, Wang M, Shi W, et al. Can fluorine-18 fluoroestradiol positron emission tomography–computed tomography demonstrate the heterogeneity of breast cancer in vivo? *Clin Breast Cancer* 2013; **13**: 359–63.
39. Judenhofer MS, Wehrl HF, Newport DF, Catana C, Siegel SB, Becker M, et al. Simultaneous PET-MRI: a new approach for functional and morphological imaging. *Nat Med* 2008; **14**: 459–65.
40. Choyke PL, Dwyer AJ, Knopp MV. Functional tumor imaging with dynamic contrast-enhanced magnetic resonance imaging. *J Magn Reson Imaging* 2003; **17**: 509–20.
41. Metz S, Ganter C, Lorenzen S, van Marwick S, Herrmann K, Lordick F, et al. Phenotyping of tumor biology in patients by multimodality multiparametric imaging: relationship of microcirculation, alphavbeta3 expression, and glucose metabolism. *J Nucl Med* 2010; **51**: 1691–8.
42. Glaus C, Rossin R, Welch MJ, Bao G. In vivo evaluation of (64)Cu-labeled magnetic nanoparticles as a dual-modality PET/MR imaging agent. *Bioconjug Chem* 2010; **21**: 715–22.
43. Fraioli F, Punwani S. Clinical and research applications of simultaneous positron emission tomography and MRI. *Br J Radiol* 2014; **87**: 20130464. doi: 10.1259/bjr.20130464
44. Langer DL, van der Kwast TH, Evans AJ, Trachtenberg J, Wilson BC, Haider MA. Prostate cancer detection with multi-parametric MRI: logistic regression analysis of quantitative T2, diffusion-weighted imaging, and dynamic contrast-enhanced MRI. *J Magn Reson Imaging* 2009; **30**: 327–34.
45. Panebianco V, Barchetti F, Sciarra A, Musio D, Forte V, Gentile V, et al. Prostate cancer recurrence after radical prostatectomy: the role of 3-T diffusion imaging in multi-parametric magnetic resonance imaging. *Eur Radiol* 2013; **23**: 1745–52.
46. Reiner CS, Stolzmann P, Husmann L, Burger IA, Hüllner MW, Schaefer NG, et al. Protocol requirements and diagnostic value of PET/MR imaging for liver metastasis detection. *Eur J Nucl Med Mol Imaging* 2014; **41**: 649–58. doi: 10.1007/s00259-013-2654-x
47. Antoch G, Bockisch A. Combined PET/MRI: a new dimension in whole-body oncology imaging? *Eur J Nucl Med Mol Imaging* 2009; **36**(Suppl. 1): S113–20. doi: 10.1007/s00259-008-0951-6
48. Wiesmüller M, Quick HH, Navalpakkam B, Lell MM, Uder M, Ritt P, et al. Comparison of lesion detection and quantitation of tracer uptake between PET from a simultaneously acquiring whole-body PET/MR hybrid scanner and PET from PET/CT. *Eur J Nucl Med Mol Imaging* 2013; **40**: 12–21. doi: 10.1007/s00259-012-2249-y
49. Chandarana H, Heacock L, Rakheja R, DeMello LR, Bonavita J, Block TK, et al. Pulmonary nodules in patients with primary malignancy: comparison of hybrid PET/MR and PET/CT imaging. *Radiology* 2013; **268**: 874–81. doi: 10.1148/radiol.13130620
50. Ohno Y, Koyama H, Yoshikawa T, Matsumoto K, Aoyama N, Onishi Y, et al. Diffusion-weighted MRI versus 18F-FDG PET/CT: performance as predictors of tumor treatment response and patient survival in patients with non-small cell lung cancer receiving chemoradiotherapy. *AJR Am J Roentgenol* 2012; **198**: 75–82.
51. Walker-Samuel S, Ramasawmy R, Torrealdea F, Rega M, Rajkumar V, Johnson SP, et al. In vivo imaging of glucose uptake and metabolism in tumors. *Nat Med* 2013; **19**: 1067–72.
52. Golman K. Molecular imaging using hyperpolarized 13C. *Br J Radiol* 2003; 76(Suppl. 2): S118–27.
53. Brindle KM, Bohndiek SE, Gallagher FA, Kettunen MI. Tumor imaging using hyperpolarized 13C magnetic resonance spectroscopy. *Magn Reson Med* 2011; **66**: 505–19.
54. Day SE, Kettunen MI, Gallagher FA, Hu DE, Lerche M, Wolber J, et al. Detecting tumor response to treatment using hyperpolarized 13C magnetic resonance imaging and spectroscopy. *Nat Med* 2007; **13**: 1382–7.
55. Nelson SJ, Kurhanewicz J, Vigneron DB, Larson PE, Harzstark AL, Ferrone M, et al. Metabolic imaging of patients with prostate cancer using hyperpolarized [1-^{13}C]pyruvate. *Sci Transl Med* 2013; **5**: 198ra108. doi: 10.1126/scitranslmed.3006070
56. Chaumeil MM, Ozawa T, Park I, Scott K, James CD, Nelson SJ, et al. Hyperpolarized 13C MR spectroscopic imaging can be used to monitor Everolimus treatment in vivo in an orthotopic rodent model of glioblastoma. *Neuroimage* 2012; **59**: 193–201.
57. Dafni H, Larson PE, Hu S, Yoshihara HA, Ward CS, Venkatesh HS, et al. Hyperpolarized 13C spectroscopic imaging informs on hypoxia-inducible factor-1 and myc activity downstream of platelet-derived growth factor receptor. *Cancer Res* 2010; **70**: 7400–10.
58. Hu S, Balakrishnan A, Bok RA, Anderton B, Larson PE, Nelson SJ, et al. 13C-pyruvate imaging reveals alterations in glycolysis that precede c-Myc-induced tumor formation and regression. *Cell Metab* 2011; **14**: 131–42. doi: 10.1016/j.cmet.2011.04.012
59. Wolfer A, Ramaswamy S. MYC and metastasis. *Cancer Res* 2011; **71**: 2034–7.
60. Berry CC, Curtis ASG. Functionalisation of magnetic nanoparticles for applications in biomedicine. *J Phys D: Appl Phys* 2003; **36**: R198–206.
61. Farokhzad OC, Langer R. Impact of nanotechnology on drug delivery. *ACS Nano* 2009; **3**: 16–20.
62. Sundstrøm T, Daphu I, Wendelbo I, Hodneland E, Lundervold A, Immervoll H, et al. Automated tracking of nanoparticle-labeled melanoma cells improves the predictive power of a brain metastasis model. *Cancer Res* 2013; **73**: 2445–56.
63. Weinstein JS, Varallyay CG, Dosa E, Gahramanov S, Hamilton B, Rooney WD, et al. Superparamagnetic iron oxide nanoparticles: diagnostic magnetic resonance imaging and potential therapeutic applications in neurooncology and central nervous system inflammatory pathologies, a review. *J Cereb Blood Flow Metab* 2010; **30**: 15–35.
64. Sarikaya I, Povoski SP, Al-Saif OH, Kocak E, Bloomston M, Marsh S, et al. Combined use of preoperative 18F FDG-PET imaging and intraoperative gamma probe detection for accurate assessment of tumor recurrence

in patients with colorectal cancer. *World J Surg Oncol* 2007; **5**: 80.
65. Epenetos AA, Kosmas C. Monoclonal antibodies for imaging and therapy. *Br J Cancer* 1989; **59**: 152–5.
66. Nieroda CA, Mojzisik C, Sardi A, Ferrara PJ, Hinkle G, Thurston MO, et al. Radioimmunoguided surgery in primary colon cancer. *Cancer Detect Prev* 1990; **14**: 651–6.
67. Nieroda CA, Mojzisik C, Hinkle G, Thurston MO, Martin EW. Radioimmunoguided surgery (RIGS) in recurrent colorectal cancer. *Cancer Detect Prev* 1991; **15**: 225–9.
68. Terwisscha van Scheltinga AG, van Dam GM, Nagengast WB, Ntziachristos V, Hollema H, Herek JL, et al. Intraoperative near-infrared fluorescence tumor imaging with vascular endothelial growth factor and human epidermal growth factor receptor 2 targeting antibodies. *J Nucl Med* 2011; **52**: 1778–85.
69. Van Dam GM, Themelis G, Crane LM, Harlaar NJ, Pleijhuis RG, Kelder W, et al. Intraoperative tumor-specific fluorescence imaging in ovarian cancer by folate receptor-α targeting: first in-human results. *Nat Med* 2011; **17**: 1315–19.
70. Kaplan RN, Rafii S, Lyden D. Preparing the "soil": the premetastatic niche. *Cancer Res* 2006; **66**: 11089–93.
71. Kaplan RN, Riba RD, Zacharoulis S, Bramley AH, Vincent L, Costa C, et al. VEGFR1-positive haematopoietic bone marrow progenitors initiate the pre-metastatic niche. *Nature* 2005; **438**: 820–7. doi: 10.1038/nature04186
72. Shokeen M, Zheleznyak A, Wilson JM, Jiang M, Liu R, Ferdani R, et al. Molecular imaging of very late antigen-4 (α4β1 integrin) in the premetastatic niche. *J Nucl Med* 2012; **53**: 779–86. doi: 10.2967/jnumed.111.100073
73. Daldrup-Link H, Coussens LM. MR imaging of tumor-associated macrophages. *Oncoimmunology* 2012; **1**: 507–9.
74. Lohela M, Bry M, Tammela T, Alitalo K. VEGFs and receptors involved in angiogenesis versus lymphangiogenesis. *Curr Opin Cell Biol* 2009; **21**: 154–65.
75. Obeid E, Nanda R, Fu YX, Olopade OI. The role of tumor-associated macrophages in breast cancer progression (review). *Int J Oncol* 2013; **43**: 5–12.
76. Pollard JW. Macrophages define the invasive microenvironment in breast cancer. *J Leukoc Biol* 2008; **84**: 623–30.
77. Tartour E, Pere H, Maillere B, Terme M, Merillon N, Taieb J, et al. Angiogenesis and immunity: a bidirectional link potentially relevant for the monitoring of antiangiogenic therapy and the development of novel therapeutic combination with immunotherapy. *Cancer Metastasis Rev* 2011; **30**: 83–95.
78. Miles DW, Chan A, Dirix LY, Cortés J, Pivot X, Tomczak P, et al. Phase III study of bevacizumab plus docetaxel compared with placebo plus docetaxel for the first-line treatment of human epidermal growth factor receptor 2-negative metastatic breast cancer. *J Clin Oncol* 2010; **28**: 3239–47.
79. Saltz LB, Clarke S, Díaz-Rubio E, Scheithauer W, Figer A, Wong R, et al. Bevacizumab in combination with oxaliplatin-based chemotherapy as first-line therapy in metastatic colorectal cancer: a randomized phase III study. *J Clin Oncol* 2008; **26**: 2013–19. doi: 10.1200/JCO.2007.14.9930
80. Burger RA, Sill MW, Monk BJ, Greer BE, Sorosky JI. Phase II trial of bevacizumab in persistent or recurrent epithelial ovarian cancer or primary peritoneal cancer: a Gynecologic Oncology Group Study. *J Clin Oncol* 2007; **25**: 5165–71.
81. Motzer RJ, Hutson TE, Tomczak P, Michaelson MD, Bukowski RM, Rixe O, et al. Sunitinib versus interferon alfa in metastatic renal-cell carcinoma. *N Engl J Med* 2007; **356**: 115–24. doi: 10.1056/NEJMoa065044
82. Llovet JM, Ricci S, Mazzaferro V, Hilgard P, Gane E, Blanc JF, et al. Sorafenib in advanced hepatocellular carcinoma. *N Engl J Med* 2008; **359**: 378–90.
83. Hirashima Y, Yamada Y, Tateishi U, Kato K, Miyake M, Horita Y, et al. Pharmacokinetic parameters from 3-Tesla DCE-MRI as surrogate biomarkers of antitumor effects of bevacizumab plus FOLFIRI in colorectal cancer with liver metastasis. *Int J Cancer* 2012; **130**: 2359–65.
84. Kelly RJ, Rajan A, Force J, Lopez-Chavez A, Keen C, Cao L, et al. Evaluation of KRAS mutations, angiogenic biomarkers, and DCE-MRI in patients with advanced non-small-cell lung cancer receiving sorafenib. *Clin Cancer Res* 2011; **17**: 1190–9. doi: 10.1158/1078-0432.CCR-10-2331
85. Barrera P, van der Laken CJ, Boerman OC, Oyen WJ, van de Ven MT, van Lent PL, et al. Radiolabelled interleukin-1 receptor antagonist for detection of synovitis in patients with rheumatoid arthritis. *Rheumatology* 2000; **39**: 870–4.
86. Barrera P, Oyen WJ, Boerman OC, van Riel PL. Scintigraphic detection of tumour necrosis factor in patients with rheumatoid arthritis. *Ann Rheum Dis* 2003; **62**: 825–8.
87. Hiratsuka S, Ishibashi S, Tomita T, Watanabe A, Akashi-Takamura S, Murakami M, et al. Primary tumours modulate innate immune signalling to create pre-metastatic vascular hyperpermeability foci. *Nat Commun* 2013; **4**: 1853.
88. Kiessling F, Farhan N, Lichy MP, Vosseler S, Heilmann M, Krix M, et al. Dynamic contrast-enhanced magnetic resonance imaging rapidly indicates vessel regression in human squamous cell carcinomas grown in nude mice caused by VEGF receptor 2 blockade with DC101. *Neoplasia* 2004; **6**: 213–23.
89. Ehling J, Lammers T, Kiessling F. Non-invasive imaging for studying anti-angiogenic therapy effects. *Thromb Haemost* 2013; **109**: 375–90. doi: 10.1160/TH12-10-0721
90. Rafii S, Lyden D. S100 chemokines mediate bookmarking of premetastatic niches. *Nat Cell Biol* 2006; **8**: 1321–3.
91. Weissleder R, Pittet MJ. Imaging in the era of molecular oncology. *Nature* 2008; **452**: 580–9.
92. Soekmadji C, Russell PJ, Nelson CC. Exosomes in prostate cancer: putting together the pieces of a puzzle. *Cancers (Basel)* 2013; **5**: 1522–44.
93. Lorentzen E, Conti E. The exosome and the proteasome: nano-compartments for degradation. *Cell* 2006; **125**: 651–4. doi: 10.1016/j.cell.2006.05.002
94. Makino DL, Halbach F, Conti E. The RNA exosome and proteasome: common principles of degradation control. *Nat Rev Mol Cell Biol* 2013; **14**: 654–60.
95. Park JE, Tan HS, Datta A, Lai RC, Zhang H, Meng W, et al. Hypoxic tumor cell modulates its microenvironment to enhance angiogenic and metastatic potential by secretion of proteins and exosomes. *Mol Cell Proteomics* 2010; **9**: 1085–99. doi: 10.1074/mcp.M900381-MCP200
96. Peinado H, Alečković M, Lavotshkin S, Matei I, Costa-Silva B, Moreno-Bueno G, et al. Melanoma exosomes educate bone marrow progenitor cells toward a pro-metastatic phenotype through MET. *Nat Med* 2012; **18**: 883–91.
97. Xiao D, Ohlendorf J, Chen Y, Taylor DD, Rai SN, Waigel S, et al. Identifying mRNA, microRNA and protein profiles of melanoma exosomes. *PLoS One* 2012; **7**: e46874.
98. Rana S, Malinowska K, Zöller M. Exosomal tumor microRNA modulates premetastatic organ cells. *Neoplasia* 2013; **15**: 281–95.
99. Kahlert C, Kalluri R. Exosomes in tumor microenvironment influence cancer progression and metastasis. *J Mol Med (Berl)* 2013; **91**: 431–7.
100. Suetsugu A, Honma K, Saji S, Moriwaki H, Ochiya T, Hoffman RM. Imaging exosome transfer from breast cancer cells to stroma at metastatic sites in orthotopic

nude-mouse models. *Adv Drug Deliv Rev* 2013; **65**: 383–90. doi: 10.1016/j.addr.2012.08.007

101. Logozzi M, De Milito A, Lugini L, Borghi M, Calabrò L, Spada M, et al. High levels of exosomes expressing CD63 and caveolin-1 in plasma of melanoma patients. *PLoS One* 2009; **4**: e5219.
102. Bergmann C, Strauss L, Wieckowski E, Czystowska M, Albers A, Wang Y, et al. Tumor-derived microvesicles in sera of patients with head and neck cancer and their role in tumor progression. *Head Neck* 2009; **31**: 371–80.
103. Kucharzewska P, Christianson HC, Welch JE, Svensson KJ, Fredlund E, Ringnér M, et al. Exosomes reflect the hypoxic status of glioma cells and mediate hypoxia-dependent activation of vascular cells during tumor development. *Proc Natl Acad Sci U S A* 2013; **110**: 7312–17.
104. Gabriel K, Ingram A, Austin R, Kapoor A, Tang D, Majeed F, et al. Regulation of the tumor suppressor PTEN through exosomes: a diagnostic potential for prostate cancer. *PLoS One* 2013; **8**: e70047. doi: 10.1371/journal.pone.0070047
105. Camacho L, Guerrero P, Marchetti D. MicroRNA and protein profiling of brain metastasis competent cell-derived exosomes. *PLoS One* 2013; **8**: e73790. doi: 10.1371/journal.pone.0073790
106. Ji H, Greening DW, Barnes TW, Lim JW, Tauro BJ, Rai A, et al. Proteome profiling of exosomes derived from human primary and metastatic colorectal cancer cells reveal differential expression of key metastatic factors and signal transduction components. *Proteomics* 2013; **13**: 1672–86.
107. Matusiak N, van Waarde A, Bischoff R, Oltenfreiter R, van de Wiele C, Dierckx RA, et al. Probes for non-invasive matrix metalloproteinase-targeted imaging with PET and SPECT. *Curr Pharm Des* 2013; **19**: 4647–72.
108. Hylton NM, Blume JD, Bernreuter WK, Pisano ED, Rosen MA, Morris EA, et al. Locally advanced breast cancer: MR imaging for prediction of response to neoadjuvant chemotherapy—results from ACRIN 6657/I-SPY TRIAL. *Radiology* 2012; **263**: 663–72.
109. Barker AD, Sigman CC, Kelloff GJ, Hylton NM, Berry DA, Esserman LJ. I-SPY 2: an adaptive breast cancer trial design in the setting of neoadjuvant chemotherapy. *Clin Pharmacol Ther* 2009; **86**: 97–100. doi: 10.1038/clpt.2009.68
110. Hylton N, Partridge S, Rosen M, Kim E, L'Heureux D, Esseman L. OT2-03-06: ACRIN 6698 MR Imaging Biomarkers for Assessment of Breast Cancer Response to Neoadjuvant Chemotherapy: A Sub-Study of the I-SPY 2 TRIAL (Investigation of Serial Studies To Predict Your Therapeutic Response with Imaging And moLecular Analysis). *Cancer Res* 2012; **71**(Suppl.).
111. Teschendorff AE, Miremadi A, Pinder SE, Ellis IO, Caldas C. An immune response gene expression module identifies a good prognosis subtype in estrogen receptor negative breast cancer. *Genome Biol* 2007; **8**: R157.
112. Ignatiadis M, Singhal SK, Desmedt C, Haibe-Kains B, Criscitiello C, Andre F, et al. Gene modules and response to neoadjuvant chemotherapy in breast cancer subtypes: a pooled analysis. *J Clin Oncol* 2012; **30**: 1996–2004. doi: 10.1200/JCO.2011.39.5624
113. Lee JD, Yun M, Lee JM, Choi Y, Choi YH, Kim JS, et al. Analysis of gene expression profiles of hepatocellular carcinomas with regard to 18F-fluorodeoxyglucose uptake pattern on positron emission tomography. *Eur J Nucl Med Mol Imaging* 2004; **31**: 1621–30.
114. Ignatius MS, Chen E, Elpek NM, Fuller AZ, Tenente IM, Clagg R, et al. In vivo imaging of tumor-propagating cells, regional tumor heterogeneity, and dynamic cell movements in embryonal rhabdomyosarcoma. *Cancer Cell* 2012; **21**: 680–93.
115. Karn T, Pusztai L, Holtrich U, Iwamoto T, Shiang CY, Schmidt M, et al. Homogeneous datasets of triple negative breast cancers enable the identification of novel prognostic and predictive signatures. *PLoS One* 2011; **6**: e28403.
116. Segal E, Sirlin CB, Ooi C, Adler AS, Gollub J, Chen X, et al. Decoding global gene expression programs in liver cancer by noninvasive imaging. *Nat Biotechnol* 2007; **25**: 675–80. doi: 10.1038/nbt1306
117. Rutman AM, Kuo MD. Radiogenomics: creating a link between molecular diagnostics and diagnostic imaging. *Eur J Radiol* 2009; **70**: 232–41.
118. Greenman C, Stephens P, Smith R, Dalgliesh GL, Hunter C, Bignell G, et al. Patterns of somatic mutation in human cancer genomes. *Nature* 2007; **446**: 153–8.
119. Koboldt DC, Fulton RS, McLellan MD, Schmidt H, Kalicki-Veizer J, McMichael JF, et al. Comprehensive molecular portraits of human breast tumours. *Nature* 2012; **490**: 61–70.
120. Nik-Zainal S, Van Loo P, Wedge DC, Alexandrov LB, Greenman CD, Lau KW, et al. The life history of 21 breast cancers. *Cell* 2012; **149**: 994–1007.
121. Arcila ME, Chaft JE, Nafa K, Roy-Chowdhuri S, Lau C, Zaidinski M, et al. Prevalence, clinicopathologic associations, and molecular spectrum of ERBB2 (HER2) tyrosine kinase mutations in lung adenocarcinomas. *Clin Cancer Res* 2012; **18**: 4910–18.
122. Perera SA, Li D, Shimamura T, Raso MG, Ji H, Chen L, et al. HER2YVMA drives rapid development of adenosquamous lung tumors in mice that are sensitive to BIBW2992 and rapamycin combination therapy. *Proc Natl Acad Sci U S A* 2009; **106**: 474–9. doi: 10.1073/pnas.0808930106
123. Dijkers EC, Oude Munnink TH, Kosterink JG, Brouwers AH, Jager PL, de Jong JR, et al. Biodistribution of 89Zr-trastuzumab and PET imaging of HER2-positive lesions in patients with metastatic breast cancer. *Clin Pharmacol Ther* 2010; **87**: 586–92. doi: 10.1038/clpt.2010.12
124. Tamura K, Kurihara H, Yonemori K, Tsuda H, Suzuki J, Kono Y, et al. 64Cu-DOTA-trastuzumab PET imaging in patients with HER2-positive breast cancer. *J Nucl Med* 2013; **54**: 1869–75. doi: 10.2967/jnumed.112.118612
125. Walsh AJ, Cook RS, Manning HC, Hicks DJ, Lafontant A, Arteaga CL, et al. Optical metabolic imaging identifies glycolytic levels, subtypes, and early-treatment response in breast cancer. *Cancer Res* 2013; **73**: 6164–74.
126. Stransky N, Egloff AM, Tward AD, Kostic AD, Cibulskis K, Sivachenko A, et al. The mutational landscape of head and neck squamous cell carcinoma. *Science* 2011; **333**: 1157–60. doi: 10.1126/science.1208130
127. Hofree M, Shen JP, Carter H, Gross A, Ideker T. Network-based stratification of tumor mutations. *Nat Methods* 2013; **10**: 1108–15.
128. Diaz LA, Williams RT, Wu J, Kinde I, Hecht JR, Berlin J, et al. The molecular evolution of acquired resistance to targeted EGFR blockade in colorectal cancers. *Nature* 2012; **486**: 537–40. doi: 10.1038/nature11219
129. Miles KA, Ganeshan B, Rodriguez-Justo M, Goh VJ, Ziauddin Z, Engledow A, et al. Multifunctional imaging signature for V-KI-RAS2 Kirsten rat sarcoma viral oncogene homolog (KRAS) mutations in colorectal cancer. *J Nucl Med* 2014; **55**: 386–91. doi: 10.2967/jnumed.113.120485